SCIENTIFIC REPORTS

OPEN

SUBJECT AREAS:
GLASSES
STRUCTURE OF SOLIDS AND LIQUIDS
SURFACES, INTERFACES AND THIN FILMS

Received
17 December 2013

Accepted
6 February 2014

Published
26 February 2014

Correspondence and requests for materials should be addressed to S.K.L. (sungklee@snu.ac.kr)

Probing of 2 dimensional confinement-induced structural transitions in amorphous oxide thin film

Sung Keun Lee[1] & Chi Won Ahn[2]

[1]Laboratory of Physics and Chemistry of Earth Materials, School of Earth and Environmental Sciences, Seoul National University, Seoul, 151-742 Korea, [2]National Nanofab Center, Korean Advanced Institute of Science and Technology, Daejeon 305-806, Korea.

Whereas the atomic structure of surface of crystals is known to be distinct from that of bulk, experimental evidence for thickness-induced structural transitions in amorphous oxides is lacking. We report the NMR result for amorphous alumina with varying thickness from bulk up to 5 nm, revealing the nature of structural transitions near amorphous oxide surfaces/interfaces. The coordination environments in the confined amorphous alumina thin film are distinct from those of bulk, highlighted by a decrease in the fractions of high-energy clusters (and thus the degree of disorder) with thickness. The result implies that a wide range of variations in amorphous structures may be identified by controlling its dimensionality.

If the atoms in an amorphous network are spatially confined into the two-dimensionally deposited thin film with thickness of ~nm [here, the state is defined as 2-dimensional (2D) confinement], the proportion of the atoms on and near the surfaces/interfaces becomes prevalent. The structure of the surface/interface of amorphous oxides under spatial confinement has remained illusive: the unsolved questions are whether the structure of the confined amorphous oxide is distinct from that of bulk analogue, if it is different, whether disorder is more prevalent with increasing 2D confinement or not. The lack of knowledge is in stark contrast to the wealth of information available on crystalline analogues, for which the structure of the surfaces are known to be often different from that of the bulk oxides (e.g.[1-4],). The knowledge gap derives from the fact that conventional surface-sensitive probes of crystals have limited usefulness for exploring the detailed short-range structures (e.g., cation coordination number) of amorphous oxides under confinement[5].

Potential structural changes in amorphous oxide due to 2D confinement have been indirectly suggested from the differences between the properties of amorphous thin films with varying thickness and those of bulk materials[6,7]. These studies, together with studies of glass surfaces, suggest that the degree of structural disorder in amorphous oxide thin film may increase with decreasing thickness[8-12]: the increase in elastic modulus of amorphous SiO_2 was attributed to an increase in the fraction of smaller-membered rings, indicating an increase in the structural disorder and defect concentration at surfaces[9-12] as also suggested for the surfaces of amorphous selenium thin film[13]. In contrast, enhanced mobility at surfaces suggested for amorphous polymer thin film (e.g.[14],) may result in a decrease in configurational disorder.

Al_2O_3, an archetypal oxide, has applications, ranging from gate microelectronic devices to flash memory components to supports for catalytic nanoparticles [e.g.[2,3,15], and references therein]. High-resolution solid-state NMR revealed that bulk amorphous Al_2O_3 consists of mostly $^{[4]}Al$, $^{[5]}Al$, and minor fraction of $^{[6]}Al$ configurations[16,17]. In order to probe the local structures under 2D confinement we collected NMR spectra for amorphous Al_2O_3 thin films that varied in deposition thicknesses up to 5 nm. Whereas ^{27}Al NMR provides a unique opportunity to resolve $^{[4,5,6]}Al$ sites in the amorphous alumina[16,17], the method is bulk sensitive and thus does not probe atoms located near surfaces selectively. However, the NMR techniques can be potentially utilized to probe spatially confined atoms in the thin film if the thin film thickness approaches to ~nm: the fraction of Al nuclear spins near the surfaces/interfaces systematically increases, enabling us to yield unambiguous Al coordination environment in the thin film under confinement. The potential results provide improved insights into the effect of thin film thickness on their properties with wider applications in microelectronic coatings. As the signal intensity decreases with decreasing film thickness, extremely low

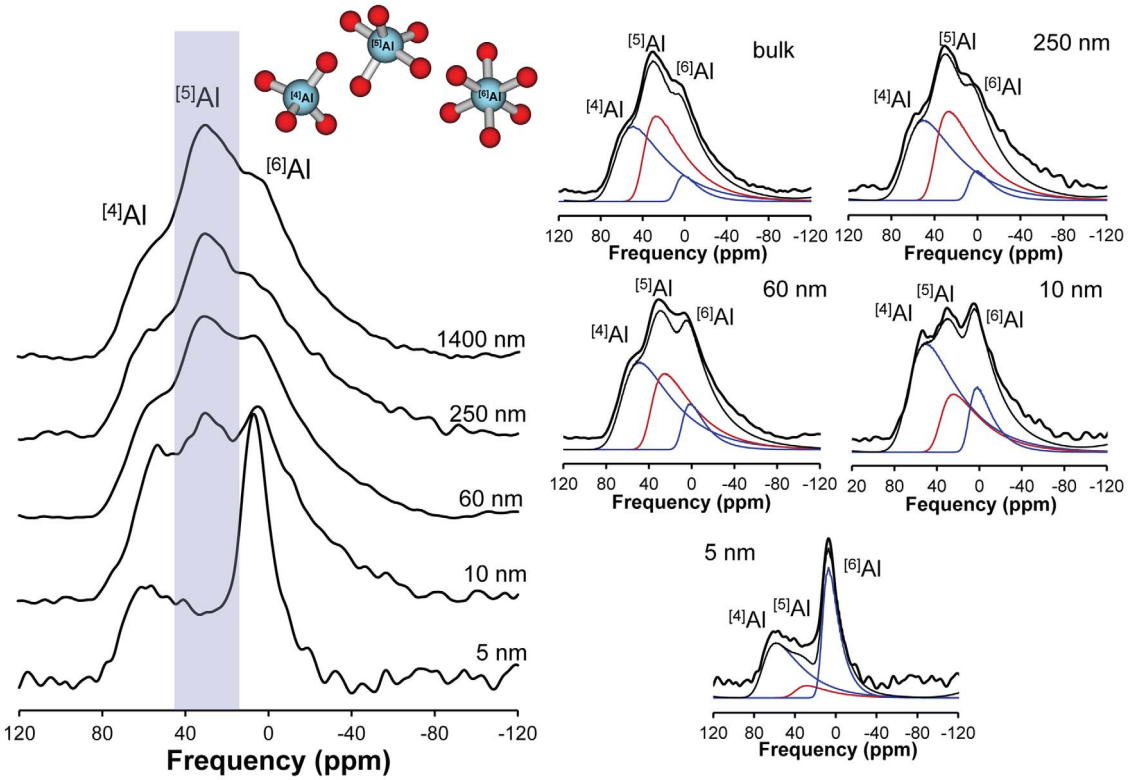

Figure 1 | (Left) ^{27}Al MAS NMR spectra of an amorphous Al_2O_3 thin film with deposition thicknesses ranging from 1.4 μm to 5 nm. The rotor backgrounds were subtracted from the spectra (see SI for further details). (Right) Simulation results for ^{27}Al MAS NMR spectra of the amorphous Al_2O_3 thin film with varying thickness as labeled. Blue lines refer to simulation result of the spectra using and the three Czjzek distribution for $^{[4,5,6]}$Al. Parameters used for simulations are shown in Table S1 (see SI).

Al nuclear spin content in thin Al_2O_3 film (~nm)/Si_3N_4 (0.5–1 μm) substrate complex pose great challenge to yield high-quality NMR spectra. Here, we report the first high-resolution solid-state NMR signal from the ~nm scale thin film, revealing the previously unknown effect of thickness on the structure and disorder amorphous oxides.

Results and Discussion

NMR results. Figure 1 (Left) shows ^{27}Al MAS NMR spectra for amorphous Al_2O_3 thin films with deposition thicknesses. Features associated with three distinct coordination environments, including $^{[4]}$Al (~60 ppm), $^{[5]}$Al (~30 ppm), and $^{[6]}$Al (~0 ppm), are partially revealed in the NMR spectra[16,18-22]. The NMR result demonstrates differences in the relative fractions of Al species with respect to thickness. Particularly, the intensity of the $^{[5]}$Al peak apparently decreases, with a decrease in thickness, and its fractions in the thinner films are smaller than that of bulk alumina. The peak shapes of amorphous thin films including 5 nm Al_2O_3 films is distinct from both the bulk amorphous alumina (1.4 μm) and crystalline polymorphs (e.g., γ-Al_2O_3)[16,23]: the 5 nm Al_2O_3 thin film shows a somewhat narrow $^{[6]}$Al peak. While this might be due to poorly crystalline phases in the interlayer or an increase in topological order in the amorphous oxide due to confinement, evidence for the crystalline phase was not found [see supplementary information (SI) figure S1 for TEM result]. Fractions of $^{[4,5,6]}$Al sites were obtained by simulating ^{27}Al MAS NMR spectra using the Czjzek distribution functions for $^{[4,5,6]}$Al sites (see SI)[24,25]. Figure 1 (Right) shows the results of a simulation. The fractions of $^{[5]}$Al and $^{[6]}$Al in the 1.4 μm alumina thin film are approximately 40% and 8%, similar to those reported from the earlier 2D NMR spectra for the identical sample[16,17]. The results clearly shows that the $^{[5]}$Al fraction decreases with decreasing thin film thickness.

Thickness-induced structural transitions and disorder in amorphous alumina thin film. The effect of thickness on the $^{[5]}$Al fraction in amorphous alumina is shown in figure 2 (Top). The $^{[5]}$Al fraction does not change significantly from 1.4 μm to 250 nm (~44%), but it gradually decreases with decreasing thickness from 250 nm, 60 nm (~37%) and up to 10 nm (~25%) while the fractions of $^{[4,6]}$Al increase. The decrease in the $^{[5]}$Al fraction is significant from 10 to 5 nm (figure 2 top, inset). Although there is uncertainty associated with the absolute fraction of each Al site (see SI, figure S4, table S1), the relative difference in the $^{[5]}$Al fraction with varying deposition thickness is clear from figure 1 and the quantification of Al sites confirms that the fraction of $^{[5]}$Al decreases with decreasing thickness.

While the difference in the fractions of Al coordination environments with varying thickness may also result from differences in the deposition conditions, the observed difference in the thin film structure at identical deposition conditions (temperature, Ar partial pressure, sputtering power, etc.) and deposition temperature and identical substrate can be attributed to the intrinsic effect of varying thickness. The results indicate that structural rearrangements near surface of amorphous thin films could be prominent for more than several nm, contributing to observed changes in the Al coordination number. These results highlight differences in cation coordination number between the bulk and amorphous oxides under 2D confinement.

The fraction of $^{[5]}$Al species in amorphous alumina is a direct measure of the extent of disorder because the structural disorder increases with the fraction of higher energy clusters[17]. A semi-quantitative, conceptual model below may provide insight into the effect of thickness on the structure. We consider a two-level system consisting of high- ($^{[5]}$Al) and low-energy configurations ($^{[4,6]}$Al) with energy difference $\Delta\varepsilon$ {energy penalty for the formation of $^{[5]}$Al =

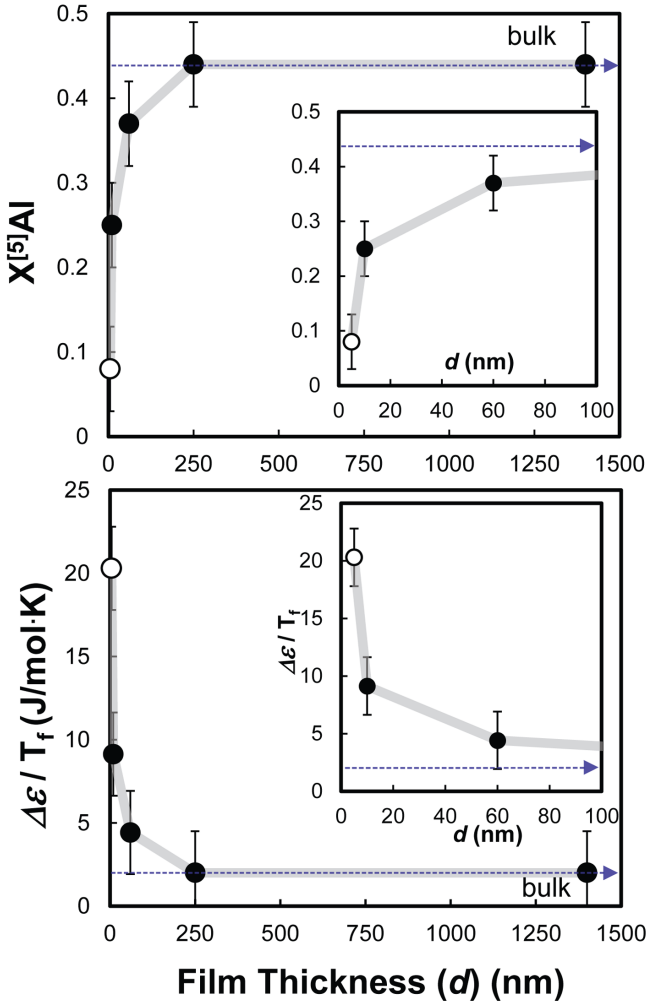

Figure 2 | (Top) Fraction of [5]Al ($X^{[5]}Al$) in amorphous Al_2O_3 thin film as a function of deposition thickness (d) from 1.4 μm to 5 nm (open circle). Thick dotted lines are [5]Al fraction in the bulk (1.4 μm) amorphous Al_2O_3. (Bottom) Energy penalty (J/mol.K) for the formation of [5]Al ($\Delta\varepsilon/T_f$) in amorphous Al_2O_3 thin film as a function of deposition thickness (d) from 1.4 μm to 5 nm (open circle). The grey trend lines are provided for visual clarity only. Thick dotted lines are [5]Al fraction in the bulk (1.4 μm) amorphous Al_2O_3.

1/2*[E(2[5]Al)-E([4]Al+[6]Al)]}: as diverse crystalline amorphous polymorphs consist only of [4,6]Al, the pronounced metastability of amorphous alumina over crystalline phases result from the significant fraction of [5]Al and the associated topological arrangement in the medium-range scale (e.g., clusters with triply coordinated oxygen, [3]O). Additionally, the quantum chemical calculations were performed to evaluate the relative stability of Al clusters: the optimized model Al-clusters include those involving [3]O cluster with two [5]Al and one [4]Al (2[5]Al-[3]O-[4]Al) and with two [4]Al and one [6]Al (2[4]Al-[3]O-[6]Al) (see SI, figures S5 and S6). The single point energy difference between clusters per Al {$\Delta\varepsilon$ = [E(2[5]Al-[3]O-[4]Al)-E(2[4]Al-[3]O-[6]Al)]/3 = 1/2*[E(2[5]Al)-E([4]Al+[6]Al)} varies from 19 to 30 kJ/mol depending on symmetry constraints used. Considering the estimated glass transition temperature (T_g) for the bulk amorphous alumina of ~ 973 K, the calculated energy differences per Al vary from ~ 20-30 J/K. The calculation result confirms that the [5]Al cluster can be considered as higher energy cluster. The degree of disorder in the amorphous oxides may be proportional to the fraction of the high-energy cluster (i.e., [5]Al), and the thickness (d)-induced mole fraction of [5]Al ($X^{[5]}Al$) can be simply described as:

$$X^{[5]}Al(T_f,d) = \frac{1}{\exp\left[\Delta\varepsilon(d)/RT_f(d)\right]+1} \quad (1)$$

where R is the gas constant and T_f is the fictitious temperature below which the amorphous states are frozen and is thus similar to T_g: amorphous oxide with varying processing histories have different concentration of high energy states, partly accounting for the changes in physical properties. T_f in Eq.1 was introduced to describe amorphous states in amorphous solids that do not undergo glass transition from melt-quenching[17]. The trend in the observed [5]Al fraction indicates that that the degree of disorder in the amorphous oxide tend to decrease with decreasing thickness. Gradual (up to 10 nm) and sudden drops up to 5 nm in the [5]Al fraction with decreasing thickness can be accounted for an increase in $\Delta\varepsilon$ and/or scaled energy penalty, $\Delta\varepsilon/T_f$ with a decrease in thickness. As shown in figure 2 (bottom), estimated energy penalty ($\Delta\varepsilon/T_f$) for the formation of [5]Al in the thin films increases with decreasing thickness from bulk value of ~2 (for 1.4 μm film) to ~20 J/mol.K (for 5 nm film). The value at the thinnest film is comparable to the calculated $\Delta\varepsilon/T_f$ from the *ab initio* calculation (see SI). We note that, despite the remarkable similarity between the estimated energy penalty and the calculated $\Delta\varepsilon$, the model shown in Eq. 1 was addressed to provide a rather conceptual description of the observed trend. Below, we discuss the potential origins in an increases in $\Delta\varepsilon/T_f$ and other factors that could contribute to the observed trend in Al coordination environment.

Effect of thickness on the energy penalty for the formation of high energy cluster and additional extrinsic factors. In addition to changes in $\Delta\varepsilon/T_f$ with thickness we note that there are additional important extrinsic factors that could affect the Al coordination states in the oxide thin film, which include the potential presence of crystalline phases and interlayers, particularly for the 5 nm thin film, and thickness-induced changes in residual stress and T_g. First, while the results for the amorphous alumina from bulk to 10 nm thin film show the intrinsic effect of thickness on the annihilation of [5]Al, potential presence of crystalline phases in the 5 nm thin film (and/or interlayer) can be implied by the relatively sharp [6]Al peak. While the possibility that formation of poorly crystalline materials at the interlayer may not be fully discarded, we note again that the evidence for the crystalline materials was not found [see SI]. Additionally, if it would exist, the sharp peak would also be shown in the other thicker films (e.g., 10 nm film), which is not the case. The TEM image showed the presence of low density interlayer (with thickness of ~ 1 nm, white arrow) between amorphous Al_2O_3 and amorphous Si_3N_4 substrate. The volume fraction of the interlayer with ~1 nm thickness between an amorphous Si_3N_4 substrate and Al_2O_3 is ~20% of that of whole thin film layers for 5 nm thin film (Figure 1). Thus, the resulting decrease in [5]Al fraction is not primarily due to the presence of the interlayer and crystallization at the interface.

Second, 2D confinement of the atoms in amorphous alumina thin film may lead to the changes in residual stress (pressure), affecting the Al coordination environment. Previous studies have shown that the variation in thickness leads to changes in residual stress within thin film (e.g.[7,26],). For example, 1 μm amorphous Al_2O_3 thin film is reported to be under compressive stress of 1.6 GPa[7] and the stress decreases with decreasing thin film thickness. The [5,6]Al fraction in oxide glasses increases with pressure above threshold pressure of ~ 3-5 GPa (i.e., [4]Al → [5,6]Al, and [5]Al → [6]Al) depending on composition[21,22,27-29]. Below the threshold pressure, change in Al coordination number is negligible. As the thickness-induced changes in Al coordination transformation in the current study is described with the formation of [4,6]Al at the expense [5]Al (2[5]Al → [4]Al + [6]Al), the observed trend in figure 1 is not mainly due to an increase in pressure in the thin film. While residual stress could induce changes in Al coordination, the pressure should be larger than

threshold pressure, which is not the case for the Al_2O_3 films studied here. Furthermore[27], Al NMR study for a bulk amorphous Al_2O_3 *via* sol-gel synthesis and the 1 μm thin film showed that their Al coordination environments are identical (Lee et al. to be published), indicating that the changes in Al coordination environment in the thin films may not result from the stress due to 2D confinement.

Finally, Al coordination environment in the oxide glasses slightly increases (though minor) with increasing T_g (Ref. 30). The T_g of the amorphous thin film of ~nm thickness may be different from that of bulk. This could potentially affect the Al coordination environment. The scaled energy penalty (with a unit of J/mol.K) in Eq.1 takes into consideration the thickness-induced changes in the T_f as well as $\Delta\varepsilon$. The estimated change in $\Delta\varepsilon/T_f$ from ~2 (for 1.4 μm film) to ~20 J/mol.K (for 5 nm film) in the amorphous alumina can be either due to changes in $\Delta\varepsilon$ and/or T_f. An order of magnitude change in $\Delta\varepsilon/T_f$ at constant $\Delta\varepsilon$ value with varying thickness necessitates T_f of the 5 nm thin film to be ~1/10 of the bulk value (~100 K), which is not plausible. Therefore, while these extrinsic factors can affect the $^{[5]}$Al fraction, the observed decrease in $^{[5]}$Al fraction is largely due to an increase in $\Delta\varepsilon$.

The increase in $\Delta\varepsilon$ for the formation of $^{[5]}$Al cluster implies that volume of amorphous networks behave as strain energy reservoirs and is required to sustain high-energy clusters: the significant fraction of $^{[5]}$Al in the amorphous Al_2O_3 necessitates the local arrangement of atoms in an extended length scale and the changes in dimension below ~nm (threshold length) may increase $\Delta\varepsilon$. The capacity of a strain energy reservoir in the glass network thus decreases by reducing dimensionality from bulk to atoms near surfaces under 2D confinement. This finding relates specifically to amorphous Al_2O_3, but the observed trend may be applicable to other amorphous networks because of the expected prevalence of scale-dependent nature of strain-energy capacity around high-energy clusters (i.e., spatial confinement in any amorphous oxides reduces its ability of the network to accommodate high energy cluster).

Implication for glass surface. We have shown the effect of thickness (thus 2D confinement) on the structure of amorphous oxide thin films. The current results and the model may have implications for glass surfaces. However, as an amorphous oxide formed *via* thin film deposition and its glass analogue quenched from melts can be distinct, further confirmation of the current proposal for diverse glass forming oxide liquids and amorphous oxide thin film is necessary. Properties of non-crystalline oxides depends on detailed thermal history and thus synthesis conditions (e.g., melt-quenching, sol-gel synthesis, and vapor deposition)[31-34]. Therefore, it is expected that their structures (glass *vs.* deposited amorphous oxides) are different in a various length scale (from atomic to textural evolution). Additionally, the lack of a bulk glassy state for Al_2O_3 due to difficulty in synthesis *via* melt-quenching poses uncertainty in the proposal of difference in the degree of disorder between bulk and glass surface. While current approach with quantitative estimation of the Al coordination environments with NMR provides unique way to probe the degree of disorder in amorphous oxide thin films, the nature of thin amorphous oxide under 2D confinement differs from its intrinsic surface. The changes in coordination states may not be present in purely intrinsic surface structure.

In conclusion, this study presents the direct experimental evidence of distinct amorphous structure and the degree of disorder of amorphous oxide under 2D confinement. The degree of disorder in the bulk oxide is expected to be larger if confined in 2D thin film, supporting a new pathway for tuning the variability of structure by controlling the thickness of the amorphous networks. Whereas the variability of structure in glass-forming liquids can be traditionally obtained by controlling the quench rate[35], the current study indicates the existence of a wide range of variations in amorphous states achieved by varying the thickness of amorphous films. The results with changes in short-range structure may explain the thickness-induced changes in the diverse properties (reactivity, catalytic ability, mechanical properties, and chemical durability) of amorphous oxide thin films. As the local coordination environments in oxides controls their overall catalytic ability, the current results suggest that the catalytic ability of an amorphous oxide (with applications, ranging from gate microelectronic devices to flash memory components to supports for catalytic nanoparticles) can be controlled by varying its dimension.

Methods

Materials. Al_2O_3 thin film with varying thickness from 5 nm to 1.4 μm was deposited on a 6 and 8-in. *p*-type amorphous Si_3N_4/Si(100) wafer by *rf* magnetron sputtering at a pressure of 5×10^{-6} Torr[16]. Sputtering was performed on an Al_2O_3 target (99.995% purity) at room temperature with an *rf* power of 500 W in an Ar environment. After Al_2O_3 deposition, the opposite side of the Si substrate was etched using a KOH solution up to ~100 μm (for 1.4 μm thin film) or mechanically grinded up to ~30 μm (for 250 nm thin film). As for thin films with less than 60 nm thickness (5 nm, 10 nm, and 60 nm), the Si substrate was removed by etching to maximize the NMR signal from the Al_2O_3 thin film. Upon etching the thin film is protected by Si_3N_4 layer. The thickness of the amorphous Si_3N_4 substrate is approximately 1 μm (for 10 nm – 1.4 μm films) and ~500 nm (for 5 nm thin film). Etching removed Si in the middle part of the wafer selectively without giving damage to the thin film side (figures S1, S2 in SI). As the thin film was deposited and processed under vacuum in an Ar environment and thus is not likely to subject to hydroxylation. Cross-section HRTEM studies showed no clear evidence of the presence of crystalline phases in the as-deposited alumina thin film (see SI). The image showed the presence of low density interlayer (with thickness of ~ 1 nm, white arrow) between amorphous Al_2O_3 and amorphous Si_3N_4 substrate.

NMR spectroscopy. ^{27}Al MAS NMR spectra were collected on a Varian 400 solid-state spectrometer (9.4 T) at a Larmor frequency of 104.23 MHz with the *rf* pulse length of 0.3 μs. A 3.2-mm zirconia rotor with a Varian double-resonance probe was used with the relaxation delay of 1 s and rotor spinning speed of 17 kHz. Up to 460,000 scans were averaged. The spectra were referenced to a 0.1 M $AlCl_3$ solution. Signals due to the background $^{[6]}$Al from the empty rotors (and spacer) + Si substrate was collected using the identical experimental conditions and then carefully subtracted to yield the final spectrum only for thin film (see SI, figure S3). In addition to the 1D MAS NMR, other NMR techniques involving dipolar coupling between nuclides may be useful to reveal the surface structure of amorphous oxide.

1. Eng, P. J. *et al.* Structure of the hydrated alpha-Al_2O_3 (0001) surface. *Science* **288**, 1029-1033 (2000).
2. Stierle, A. *et al.* X-ray diffraction study of the ultrathin Al_2O_3 layer on NiAl(110). *Science* **303**, 1652-1656 (2004).
3. Kresse, G. *et al.* Structure of the ultrathin aluminum oxide film on NiAl(110). *Science* **308**, 1440-1442 (2005).
4. Farias, D. & Rieder, K. H. Atomic beam diffraction from solid surfaces. *Reports on Progress in Physics* **61**, 1575-1664 (1998).
5. Greaves, G. N. & Sen, S. Inorganic glasses, glass-forming liquids and amorphizing solids. *Adv. Phys.* **56**, 1-166 (2007).
6. Ao, Z. M. & Li, S. Temperature- and thickness-dependent elastic moduli of polymer thin films. *Nanoscale Res. Lett.* **6**, 243 (2011).
7. Fujiyama, H., Sumomogi, T. & Nakamura, M. Effect of O-2 gas partial pressure on mechanical properties of Al_2O_3 films deposited by inductively coupled plasma-assisted radio frequency magnetron sputtering. *J. Vac. Sci. Technol. A* **30**, 051511 (2012).
8. Steurer, W. *et al.* Surface dynamics measurements of silica glass. *Phys. Rev. B* **78**, 042457 (2008).
9. Roder, A., Kob, W. & Binder, K. Structure and dynamics of amorphous silica surfaces. *J. Chem. Phys.* **114**, 7602-7614 (2001).
10. Fan, H. Y. *et al.* Modulus-density scaling behaviour and framework architecture of nanoporous self-assembled silicas. *Nat. Mater.* **6**, 418-423 (2007).
11. Cabriolu, R. & Ballone, P. Thermodynamic properties and atomistic structure of the dry amorphous silica surface from a reactive force field model. *Phys. Rev. B* **81**, 155432 (2010).
12. Lacks, D. J. & Robinson, M. P. Mechanical heterogeneity in nanoscale films of liquid silica. *Phys. Rev. E* **77**, 041504 (2008).
13. Scopigno, T. *et al.* Vibrational dynamics and surface structure of amorphous selenium. *Nat. Commun.* **2**, 1197 (2011).
14. Sun, Y., Zhu, L., Kearns, K. L., Ediger, M. D. & Yu, L. A. Glasses crystallize rapidly at free surfaces by growing crystals upward. *Proc. Natl. Acad. Sci. U. S. A.* **108**, 5990-5995 (2011).
15. Kwak, J. H. *et al.* Coordinatively unsaturated Al^{3+} centers as binding sites for active catalyst phases of platinum on gamma-Al_2O_3. *Science* **325**, 1670-1673 (2009).
16. Lee, S. K., Lee, S. B., Park, S. Y., Yi, Y. S. & Ahn, C. W. Structure of amorphous aluminum oxide. *Phys. Rev. Lett.* **103**, 095501 (2009).

17. Lee, S. K., Park, S. Y., Yi, Y. S. & Moon, J. Structure and disorder in amorphous alumina thin films: Insights from high-resolution solid-state NMR. *J. Phys. Chem. B.* **114**, 13890-13894 (2010).
18. Smith, M. E. Application of Al-27 NMR techniques to structure determination in solids. *Appl. Mag. Res.* **4**, 1-64 (1993).
19. Baltisberger, J. H., Xu, Z., Stebbins, J. F., Wang, S. & Pines, A. Triple-quantum two-dimensional ^{27}Al magic-angle spinning nuclear magnetic resonance spectroscopic study of aluminosilicate and aluminate crystals and glasses. *J. Am. Chem. Soc.* **118**, 7209-7214 (1996).
20. Stebbins, J. F., Kroeker, S., Lee, S. K. & Kiczenski, T. J. Quantification of five- and six-coordinated aluminum in aluminosilicate and fluoride-containing glasses by high-field, high resolution ^{27}Al NMR. *J. Non-Cryst. Solids* **275**, 1-6 (2000).
21. Lee, S. K. Simplicity in melt densification in multi-component magmatic reservoirs in earth's interior revealed by multi-nuclear magnetic resonance. *Proc. Nat. Aca. Sci. USA* **108**, 6847-6852 (2011).
22. Yarger, J. L. *et al.* Al coordination changes in high-pressure aluminosilicate liquids. *Science* **270**, 1964-1967 (1995).
23. Fitzgerald, J. J., Piedra, G., Dec, S. F., Seger, M. & Maciel, G. E. Dehydration studies of a high-surface-area alumina (pseudo-boehmite) using solid-state H-1 and Al-27 NMR. *J. Am. Chem. Soc.* **119**, 7832-7842 (1997).
24. Neuville, D. R., Cormier, L. & Massiot, D. Al environment in tectosilicate and peraluminous glasses: A Al-27 MQ-MAS NMR, Raman, and XANES investigation. *Geochim. Cosmochim. Acta* **68**, 5071-5079 (2004).
25. Massiot, D. *et al.* Modelling one- and two-dimensional solid-state NMR spectra. *Mag. Res. Chem.* **40**, 70-76 (2002).
26. Thornton, J. A. & Hoffman, D. W. Stress-related effects in thin films. *Thin Solid Films* **171**, 5-31 (1989).
27. Allwardt, J. R., Poe, B. T. & Stebbins, J. F. The effect of fictive temperature on Al coordination in high-pressure (10 GPa) sodium aluminosilicate glasses. *Am. Miner.* **90**, 1453-1457 (2005).
28. Lee, S. K. The structure of silicate melts at high pressure: Quantum chemical calculations and solid state NMR. *J. Phys. Chem. B* **108**, 5889-5900 (2004).
29. Lee, S. K. Effect of pressure on structure of oxide glasses at high pressure: Insights from solid-state NMR of quadrupolar nuclides. *Solid State Nucl. Magn. Reson.* **38**, 45-57 (2010).
30. Stebbins, J. F., Dubinsky, E. V., Kanehashi, K. & Kelsey, K. E. Temperature effects on non-bridging oxygen and aluminum coordination number in calcium aluminosilicate glasses and melts. *Geochim. Cosmochim. Acta* **72**, 910-925 (2008).
31. Dussauze, M. *et al.* Structure and optical properties of amorphous lead-germanate films developed by pulsed-laser deposition. *J. Chem. Phys.* **127**, 034704 (2007).
32. Inoue, S. *et al.* Advanced approaches to functional glasses. *J. Non-Cryst. Solids* **352**, 632-645 (2006).
33. Kamitsos, E. I., Dussauze, M., Varsamis, C. P. E., Vinatier, P. & Hamon, Y. Thin film amorphous electrolytes: Structure and composition by experimental and simulated infrared spectra. *J. Phys. Chem. C* **111**, 8111-8119 (2007).
34. Exarhos, G. J. & Hess, N. J. Phase transformation dynamics, melting and stress evolution in dielectric films and at surfaces. *J. Raman Spectrosc.* **27**, 765-774 (1996).
35. Elliot, S. R. *Physics of amorphous materials.* (John Wiley & Sons, 1988).

Acknowledgments

This work was mainly supported by the National Research Foundation, Korea to S.K.L. (2012-026-411). Thin film synthesis was supported by MEST (No.2012054560) to C.W.A. We thank Saebom Ryu for help with NMR experiment and Sung Bo Lee for helpful discussion.

Additional information

Supplementary information accompanies this paper at http://www.nature.com/scientificreports

Competing financial interests: The authors declare no competing financial interests.

How to cite this article: Lee, S.K. & Ahn, C.W. Probing of 2 dimensional confinement-induced structural transitions in amorphous oxide thin film. *Sci. Rep.* **4**, 4200; DOI:10.1038/srep04200 (2014).